SUPPLEMENTARY DATA

SUPPLEMENTARY MATERIAL AND METHODS

Antibodies. H3ac (Upstate, 06-599), HIRA (Abcam, ab20655).

PP32/histone binding. 0.15 ug of recombinant His-tagged PP32 was incubated with 2.0 ug of recombinant histone H4 1 h, after which Ni^{2+}-agarose beads were added to the reaction and incubated 1 h at 4^0C. Beads were washed with a buffer containing 50mM NaCl and 0.1% NP40. Bound proteins were loaded onto 15% SDS-PAGE and analyzed by Western blot.

Histone deposition assay. The assay was performed as previously described (1). In brief, we added 10 uM of SNAP-CellBlock (Biolabs) for 30 min to quench SNAP-tag activity and then performed a 2 hr chase step in complete medium. After *in vivo* labeling with SNAP-Cell TMR-Star (Biolabs) for 20 min, we pre-extracted cells with Triton before fixation to allow the visualization of new incorporated H3-SNAP by fluorescent microscopy. Quantification of mean fluorescence intensity has been done as previously described (1,2) with minor modifications. EdU was added during pulse stage allowing visualization of replicating cells with Click-It technology (Life Technologies). For H3.1 cell line, only EdU positive nuclei have been considered for TMR fluorescence quantification whereas all the nuclei were quantified for H3.3.

SUPPLEMENTARY FIGURE LEGEND

Supplementary Figure 1. Purification of PP32, SET/TAF-Iβ, H4 and HAT1. Coomassie blue stained gel of purified recombinant PP32 (A), SET/TAF-Iβ (B), and histone H4 (C), and increasing amount of BSA, as indicated. FT corresponds to the flow thought material of the Ni^{+2}-beads for SET/TAF-Iβ purification. * Contaminant band. (D) Coomassie blue stained gel of native purified HAT1, as indicated. S100, cytosolic HeLa extract. (E) Western blot of recombinant PP32, SET/TAF-Iβ, H4, and native HAT1, as indicated. (F) Top, scheme illustrating the His-PP32 pull-down assay. Bottom, Western blot of the pull-down assay. (G) Western blot analysis on the histone acetyltransferase assay using recombinant histone H4 as substrate and increasing amounts of purified HAT1 as the enzyme source. Of note, the level of H4K12ac observed when no HAT1 was added likely corresponds to non-enzymatic acetylation (3). On the right, graph showing the H4K12ac signal quantitation, taking the -H4 condition as background. The graph shows that the signal is lineal.

Supplementary Figure 2. PP32 and SET/TAF-Iβ knock down does not affect the newly synthesized H3 acetylation levels. Western blots of 10 and 30 ug of S100 extract derived from either siControl and siPP32 treated HeLa cells, as indicated.

Supplementary Figure 3. H4 acetylation blocks the association between H4 and Hsp90. Emission intensity spectra of intrinsic protein fluorescence of recombinant HSP90 in the presence of increasing concentrations of full length recombinant H4 proteins (Top), unmodified recombinant H4 peptide (pepH4(1-20)) (middle), or tetra-acetylated H4 peptide (bottom). A saturating dose-response quenching effect of HSP90 fluorescence emission at 370 nm upon excitation at 280 nm (Trp and Tyr mainly) was observed with full length and non-modified H4 peptide. Emission intensity at peak and integration of fluorescence spectra was used for calculations of relative changes fluorescence emission and binding constants.

Supplementary Figure 4. PP32 knock-down affects histone deposition. (A) Western blot analysis of crude cell extracts from siControl, siPP32, and siHIRA treated cells. (B) Fluorescent microscopy visualization of H3.1- and H3.3-SNAP after *in vivo* labeling assays with red fluorescent TMR-Star in quench-chase-pulse experiments, to label new H3-SNAP synthesized during the 2 h chase. The replicating cells are visualized in green (EdU positive). Scale bars represent 10 nm. (C) Box plot of the TMR intensity for H3.1 and H3.3 histones. Cells were visualized by fluorescent microscopy of H3.1- and H3.3-SNAP after *in vivo* labeling assays with red fluorescent TMR-Star in quench-chase-pulse experiments, to label new H3-SNAP synthesized during the 2 h chase. Error bars indicate standard deviation in at least 3 experiments. A Mann Whitney statistical test established the significance of the difference between siControl and siPP32 for H3.1 ($p < 3.6 \times 10^{-13}$) and H3.3 ($p < 2.2 \times 10^{-16}$).

REFERENCES

1. Ray-Gallet, D., Woolfe, A., Vassias, I., Pellentz, C., Lacoste, N., Puri, A., Schultz, D.C., Pchelintsev, N.A., Adams, P.D., Jansen, L.E. *et al.* (2011) Dynamics of histone H3 deposition in vivo reveal a nucleosome gap-filling mechanism for H3.3 to maintain chromatin integrity. *Molecular cell*, **44**, 928-941.
2. Clement, C., Vassias, I., Ray-Gallet, D. and Almouzni, G. (2016) Functional Characterization of Histone Chaperones Using SNAP-Tag-Based Imaging to Assess De Novo Histone Deposition. *Methods in enzymology*, **573**, 97-117.
3. Choudhary, C., Weinert, B.T., Nishida, Y., Verdin, E. and Mann, M. (2014) The growing landscape of lysine acetylation links metabolism and cell signalling. *Nature reviews. Molecular cell biology*, **15**, 536-550.

Supplementary Figure 1: Purification of PP32, SET/TAF-Iβ, H4 and HAT1

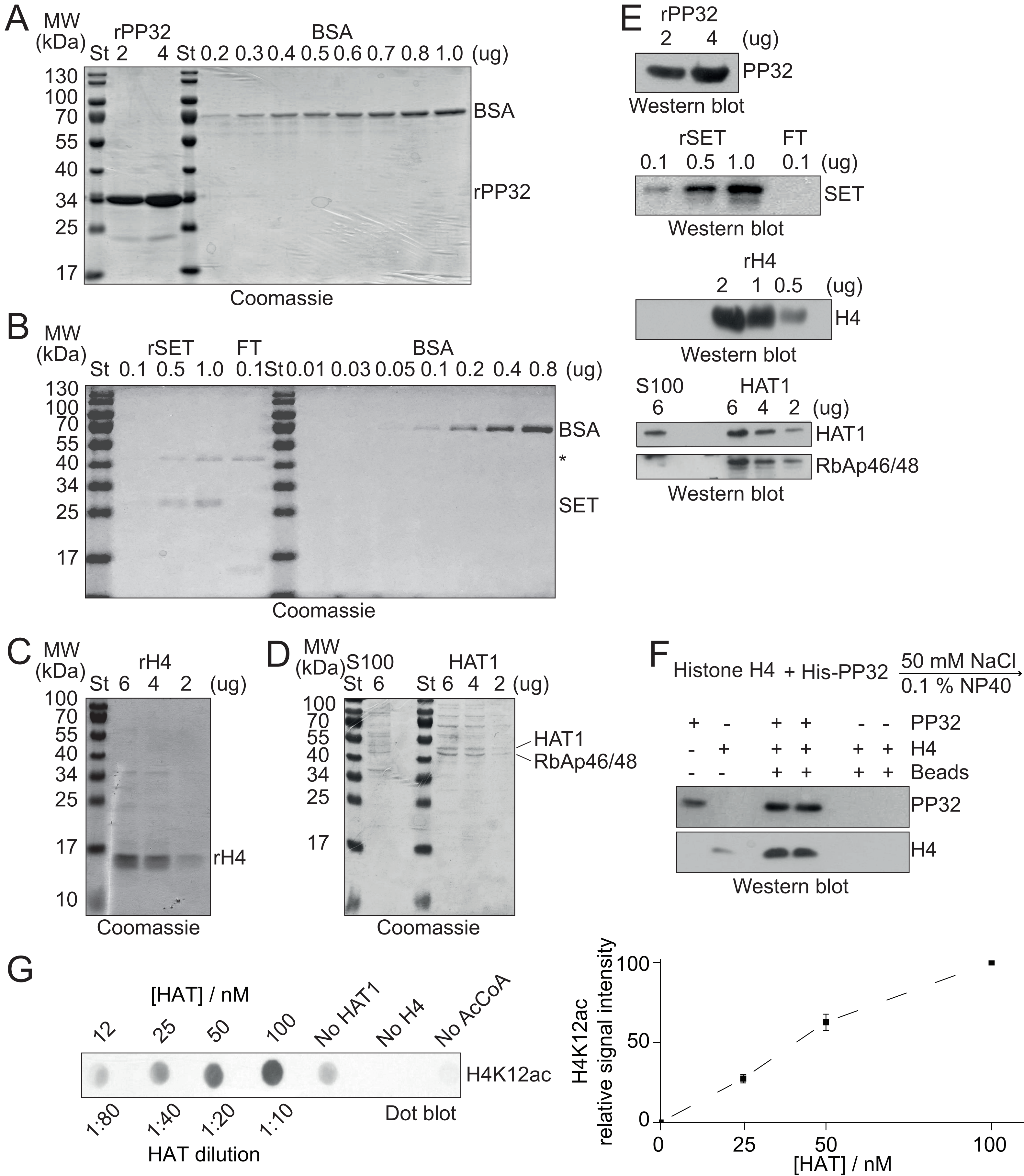

Supplementary Figure 2: PP32 and SET/TAF-Iβ knock down does not affect the newly synthesized H3 acetylation levels

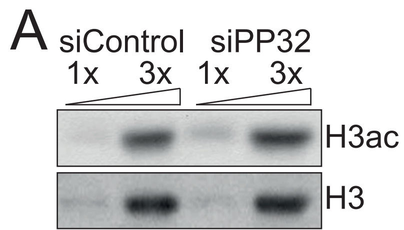

Supplementary Figure 3: H4 acetylation blocks the association between H4 and Hsp90

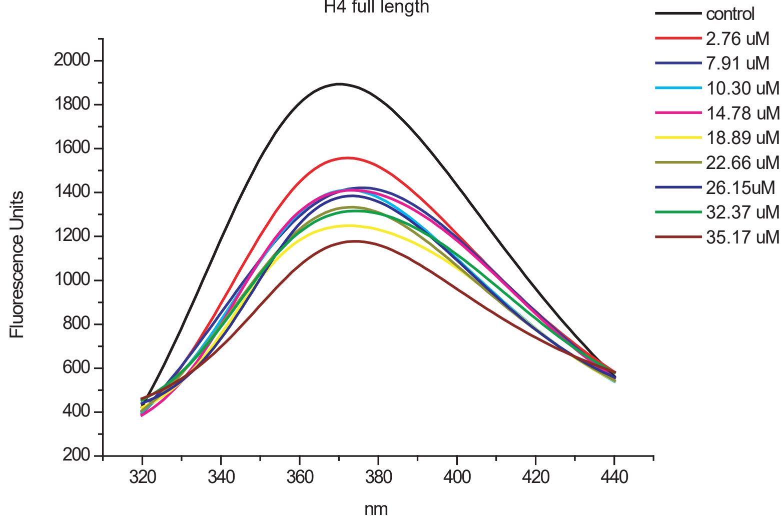

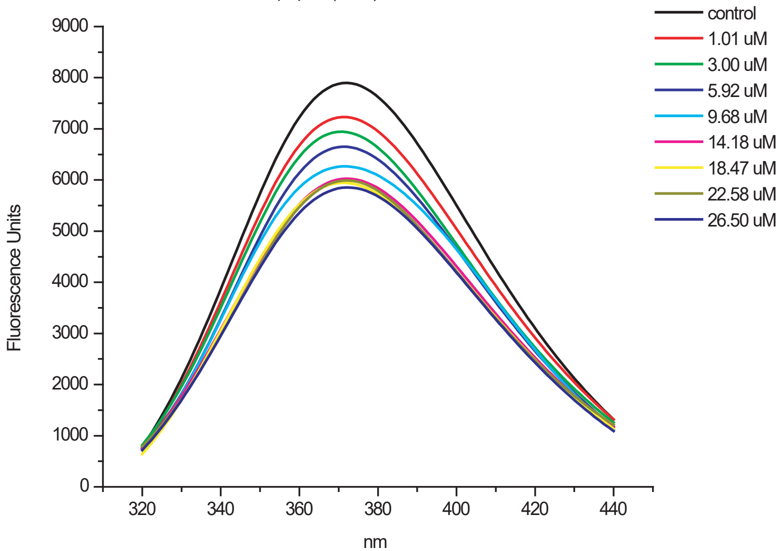

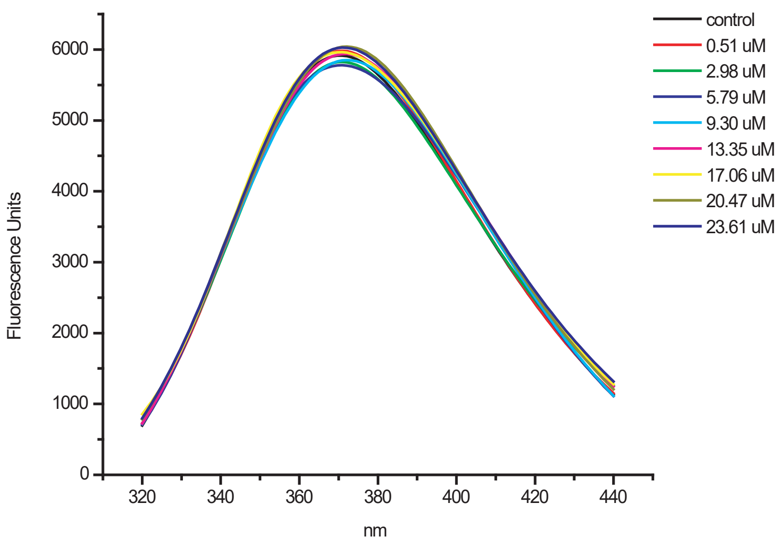

Supplementary Figure 4: PP32 knock-down affects histone deposition

A

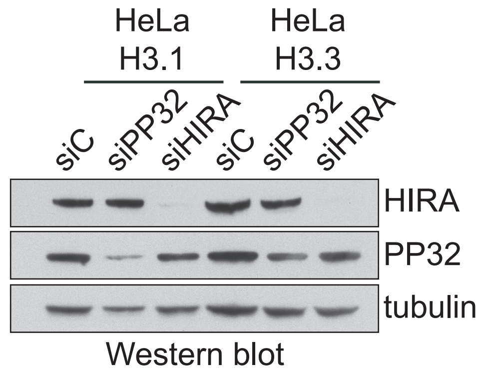

B

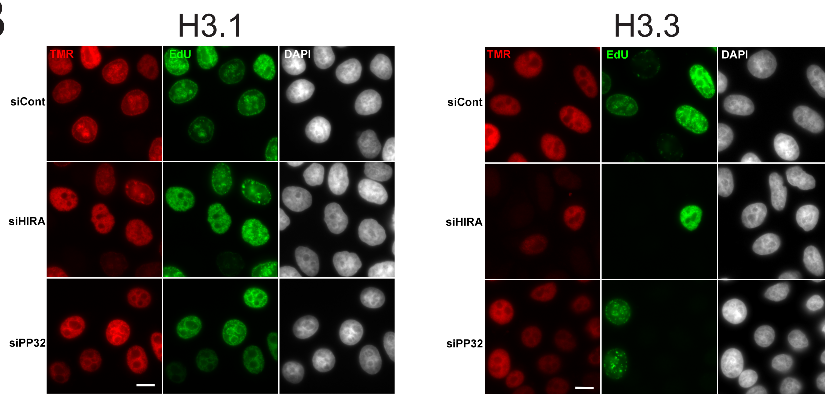

C